Theory of Electromotive Force Induced by Domain Wall Motion

Shengyuan A. Yang, Di Xiao, and Qian Niu
Department of Physics, The University of Texas, Austin, Texas, 78712-0264, USA
(Dated: March 12, 2008)

We formulate a theory on the dynamics of conduction electrons in the presence of moving magnetic textures in ferromagnetic materials. We show that the variation of local magnetization in both space and time gives rise to topological fields, which induce electromotive forces on the electrons. Universal results are obtained for the emf induced by both transverse and vortex domain walls traveling in a magnetic film strip, and their measurement may provide clear characterization on the motion of such walls.

PACS numbers: 75.75.+a 72.25.Ba 75.47.-m 75.60.Ch

The interplay between electron transport and magnetic dynamics is a central problem of spintronics research. It has been known that the presence of a domain wall (DW) can change the electrical resistance of a ferromagnetic conductor [1, 2, 3, 4]. It has also been demonstrated that an electric current can drive a DW through coupling between the conduction electrons and the local magnetic moments [5, 6, 7, 8, 9, 10, 11, 12, 13, 14, 15]. The reverse of this effect, i.e., electron transport induced by a moving DW, has been proposed by Berger [16] based on phenomenological arguments about twenty years ago. Recently there is renewed interest in this effect and the result for 1D transverse domain wall has been derived rigorously using various approaches [17, 18, 19], connecting to Berry phase effects on electron spins in a magnetic texture [20, 21, 22]. However, realistic DW profiles and their motion are far more complicated than the simple 1D model [23, 24], typically involving vortices. So a general microscopic theory applicable to higher dimensions is very much desired.

In this Letter, we provide such a theory within the framework of semiclassical dynamics of electrons in a magnetic background which varies slowly in both space and time. Indeed, the width of a typical DW in a ferromagnetic nanowire is about a few hundred nanometers, which is much larger than the electron Fermi wavelength, and the DW speed is much smaller than the electron speed. One can therefore consider the semiclassical formalism with adiabatic approximation where the spin of the conduction electron follows the direction of local spin vector. We find that Berry phase terms [20] enter into the equation of motion as a pair of topological fields, acting locally like electric and magnetic fields on the electrons.

While our theory naturally reproduces previous results on 1D transverse walls, we consider carefully the effect of a moving vortex wall. We predict both longitudinal and transverse voltage with universal results which may be used to provide clear characterization of the wall motion. Extra voltage due to nonadiabatic effects is also estimated at the end of the paper, and is found to be subdominant.

To construct our theory, we consider a ferromagnetic thin film, which is taken to be the x-y plane. The time evolution of local magnetization can be driven by a uniform applied magnetic field (x-direction). Our model Hamiltonian then takes the following form,

$$H = H_0[\boldsymbol{q} + (e/\hbar)\boldsymbol{A}(\boldsymbol{r})] - J\hat{\boldsymbol{n}}(\boldsymbol{r},t)\cdot\boldsymbol{\sigma} - h\sigma_x. \quad (1)$$

The first term is the bare Hamiltonian for a conduction electron, $\boldsymbol{q}$ is the Bloch wave-vector, and $\boldsymbol{A}(\boldsymbol{r})$ is the vector potential of the external magnetic field. The second term is the s-d coupling between a conduction electron and the local d-electron spin along direction $\hat{\boldsymbol{n}}(\boldsymbol{r},t)$, and J is the s-d coupling strength. The last term represents the Zeeman coupling between electron and the external magnetic field, with $h = \frac{1}{2}g_s\mu_B B$.

To apply the semiclassical wave-packet formalism for the conduction electrons [25], we first write down the local Hamiltonian at the center position of the electron wave-packet $\boldsymbol{r}_c$,

$$H_c = H_0[\boldsymbol{q} + (e/\hbar)\boldsymbol{A}(\boldsymbol{r}_c)] - K(\boldsymbol{r}_c,t)\hat{\boldsymbol{n}}'(\boldsymbol{r}_c,t)\cdot\boldsymbol{\sigma}, \quad (2)$$

where $\hat{\boldsymbol{n}}'(\boldsymbol{r}_c,t)$ is the unit vector of the exchange plus Zeeman field, while $K(\boldsymbol{r}_c,t)$ is its strength. As discussed by Sundaram and Niu [25], we introduce the gauge invariant crystal momentum $\boldsymbol{k} = \boldsymbol{q} + (e/\hbar)\boldsymbol{A}(\boldsymbol{r})$. For now, we only consider the majority carriers whose spins are polarized along $\hat{\boldsymbol{n}}'(\boldsymbol{r}_c,t)$, and spin minority carriers are considered in the end. The position and time dependence of the spinor wave function gives rise to Berry curvatures in space and time, which can affect the dynamics of an electron wavepacket. More specifically, we find that the equations of motion for the wavepacket center are (subscript c is dropped here)

$$\dot{\boldsymbol{r}} = \frac{\partial\mathcal{E}_0}{\hbar\partial\boldsymbol{k}}, \quad (3)$$

$$\dot{\boldsymbol{k}} = \frac{\partial K}{\hbar\partial\boldsymbol{r}} - \frac{e}{\hbar}\dot{\boldsymbol{r}}\times\boldsymbol{B} - \dot{\boldsymbol{r}}\times\boldsymbol{C} - \boldsymbol{D}, \quad (4)$$

where $\mathcal{E}_0$ is the Bloch band energy obtained from H_0. Originated from Berry curvatures in real space and time,

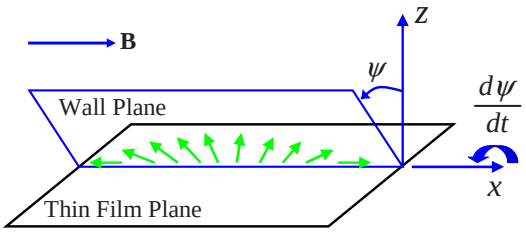

FIG. 1: (color online). Schematic picture of a transverse domain wall. The local spin direction changes within a wall plane which makes an angle ψ with the vertical direction.

two new fields $\boldsymbol{C}$ and $\boldsymbol{D}$ appear in the equations of motion. They are entirely due to the spatial and temporal variation of local spin textures. In terms of the spherical angles (θ, ϕ) specifying the direction of $\hat{\boldsymbol{n}}'$, the fields $\boldsymbol{C}$ and $\boldsymbol{D}$ are given by

$$\boldsymbol{C}(\boldsymbol{r}, t) \equiv \frac{1}{2} \sin\theta \left(\nabla\theta \times \nabla\phi\right), \tag{5}$$

$$\boldsymbol{D}(\boldsymbol{r}, t) \equiv \frac{1}{2} \sin\theta \left(\frac{\partial\phi}{\partial t}\nabla\theta - \frac{\partial\theta}{\partial t}\nabla\phi\right). \tag{6}$$

Field $\boldsymbol{C}$ is similar to the gyrovector used in the discussion of Bloch line dynamics [26]. From their appearance in equation (4), we observe that $\boldsymbol{C}$ acts like a magnetic field while $\boldsymbol{D}$ behaves like an electric field. We note that our theory applies locally to the dynamics of electrons, while recent work of Ref.[17, 18] focuses more on the global aspect of Berry phase effects.

Next we apply these formulas to the one-dimensional domain wall case where θ and ϕ only depend on coordinate x of the 2D plane. We then have $\boldsymbol{C} = 0$ and $\boldsymbol{D} = D\hat{\boldsymbol{e}}_x$. For a transverse domain wall in the absence of external magnetic field, the local spins rotate within the 2D plane with the profile $\theta = \pi/2$ and $\phi(x) = \cos^{-1}\tanh[(x - X)/\lambda]$, where X denotes the center of the DW and λ is the DW width [26]. When an external $\mathbf{B}$ field is applied, not only will the DW propagate, but the local spins will also get tilted out of the x-y plane. As shown in Fig.1, these spins still lie within a "wall plane" which makes an angle ψ with the vertical direction. Below Walker's breakdown field, this plane is fixed, and the angles θ and ϕ are functions of $(x - vt)$, which makes $\boldsymbol{D} = 0$. Above Walker's breakdown field, this plane changes with time (with rate denoted by $d\psi/dt$) [26], which leads to a non-zero $\boldsymbol{D}$ field.

If the system is bounded electrically, in a steady state, the DW motion induced adiabatic force $\hbar(\partial K/\hbar\partial x - D)$ must be balanced by the gradient of electrochemical potential. The emf along the direction of DW motion, which is the measured voltage change, is given by

$$V_x = \frac{\hbar}{e}\int\left(\frac{\partial K}{\hbar\partial x} - D\right)\mathrm{d}x = \frac{\hbar}{e}\left(\frac{\mathrm{d}\psi}{\mathrm{d}t} + \frac{2h}{\hbar}\right). \tag{7}$$

In the calculation, we use the condition $|h| \ll |J|$, which is usually the case in experiments on ferromagnetic materials. The first term on the right hand side represents the so-called *AC ferro-Josephson effect* proposed by Berger in 1986 based on phenomenological considerations [16]. More careful analyses on this effect have been done recently using different approaches [17, 18, 19]. The additional term proportional to the field is due to the difference in Zeeman energy on the two sides of the DW, which should appear when we suddenly turn on the external field. However, since the spin relaxation time $\tau_s \sim 10^{-12}$s is much shorter than the characteristic time for DW motion, the voltage associated with this term cannot be measured in experiment [27].

Depending on the thickness and the width of the system, a stable DW in a thin film can also take a vortex structure [23, 24]. In fact, most of the experiments done so far involve vortex walls rather than transverse walls. In the following, we apply the formula developed above to study the case of a single vortex in a nanowire. Assume that the vortex profile is characterized by a core radius a, which is about a few nanometers, and an outer radius R, which is comparable to the wire width w. For a vortex centered at $\boldsymbol{X}(t)$, we may approximately write $\theta = \frac{\pi}{2}\left[1 - p\exp(-|\boldsymbol{r} - \boldsymbol{X}(t)|/a)\right]$ for $|\boldsymbol{r} - \boldsymbol{X}| < R$ and $\theta = \frac{\pi}{2}$ beyond the outer radius, $p = \pm 1$ is the polarization. In both cases, we have $\phi = q\arg(\boldsymbol{r} - \boldsymbol{X}(t)) + c\frac{\pi}{2}$ for $|\boldsymbol{r} - \boldsymbol{X}| < R$, where $q = \pm 1$ is the vorticity of the vortex ($q = -1$ is also referred to as antivortex in literature [30]), and $c = \pm 1$ indicates its chirality. For a steady state motion of the vortex, θ and ϕ are functions of $(\boldsymbol{r} - \boldsymbol{v}t)$, where $\boldsymbol{v} = \dot{\boldsymbol{X}}$. Then

$$\boldsymbol{D} = -\frac{1}{2}\sin\theta\left[(\boldsymbol{v}\cdot\nabla\phi)\nabla\theta - (\boldsymbol{v}\cdot\nabla\theta)\nabla\phi\right] = \boldsymbol{C}\times\boldsymbol{v}, \tag{8}$$

which resembles the relation between $\boldsymbol{E}$ and $\boldsymbol{B}$ fields. Because $a \ll R \sim w$, these fields are concentrated within the core region, where

$$\boldsymbol{C} = pq\frac{\pi}{4ar}e^{-r/a}\cos\left(\frac{\pi}{2}e^{-r/a}\right)\hat{\boldsymbol{e}}_z, \tag{9}$$

and $\boldsymbol{D}$ is obtained by Eq.(8). An important property of the $\boldsymbol{C}$ field is that its total flux is a constant, i.e.,

$$\int \boldsymbol{C}d^2r = \frac{1}{2}\int \sin\theta d\theta d\varphi\hat{\boldsymbol{e}}_z = pq\pi\hat{\boldsymbol{e}}_z. \tag{10}$$

which is topologically invariant—independent of the detailed profile of the vortex.

The two-dimensional character of the vortex domain wall makes the calculation of the induced voltage a bit complicated. Unlike the one-dimensional transverse wall case, the force field $\boldsymbol{D}$ now has a curl. The gradient of the electrochemical potential can only cancel the longitudinal part of this force field. Therefore, we need to solve the Poisson equation $\nabla^2 V = (\hbar/e)\nabla\cdot\boldsymbol{D}$ with Neumann boundary condition (no current leaving the sample). It

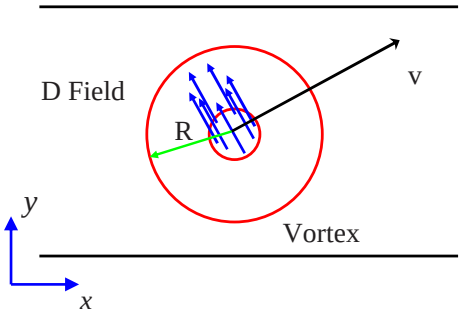

FIG. 2: (color online). Schematic picture of the $\boldsymbol{D}$ field for a moving vortex. $\boldsymbol{D}$ field is perpendicular to the vortex velocity and concentrated within the vortex core.

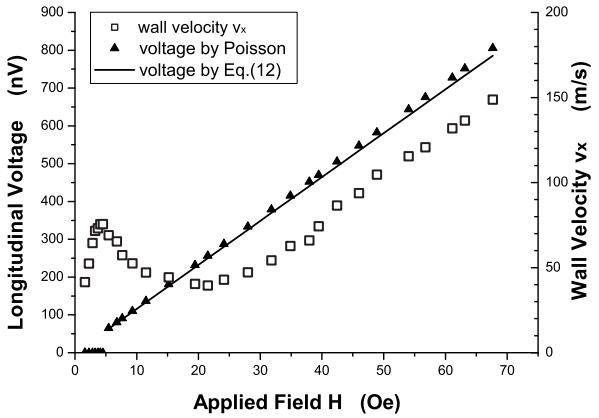

FIG. 3: Numerical results for longitudinal DC voltage associated with the vortex motion. The triangular data points are obtained by directly solving the Poisson equation with $\bar{v}_y = \gamma H w/\pi$ for the sample used in Beach et al.'s experiment [33]. For comparison, a solid line is drawn based on Eq.(12). Here also shows the mobility curve measured experimentally in Ref.[33].

is seen that the effect of the $\boldsymbol{D}$ field may be regarded as that of an electric dipole $\mathbf{P}$, whose spatial extension is of the size of the core. The net dipole moment is equivalently given by the integral of the $\boldsymbol{D}$ field times $\hbar\varepsilon_0/e$. With the help of Eq.(8) and (10), $\mathbf{P} = pq\varepsilon_0\pi(\hbar/e)\hat{\boldsymbol{e}}_z \times \boldsymbol{v}$, which is also a topological property of the vortex.

Another complication arises from the Magnus force on a moving vortex which pushes it in the direction perpendicular to its velocity [28]. At low fields, this Magnus force is balanced by the confining potential of the nanowire such that steady motion is still along x-direction. In this case, the source term of the Poisson equation resembles an electric dipole pointing along the y-direction, so the longitudinal voltage is expected to vanish in this case (baring nonadiabatic effects).

Above the breakdown field, the confining potential can no longer balance the Magnus force and the vortex will begin a transverse motion [13, 29, 30, 31]. When its core hits one edge, the vortex domain wall transforms into a transverse wall. There is a range of external field under which this transverse wall propagates and generates a voltage according to Eq.(7). But more probably, another vortex with reversed polarization will be emitted from the edge, travel across the wire and hit the other edge. These transformations continue periodically as the DW moves along the wire [31].

When the vortex begins transverse motion, from the relation $\boldsymbol{D} = \boldsymbol{C} \times \boldsymbol{v}$, we observe that the dipole source gets rotated to acquire a finite x component. This makes the longitudinal voltage nonzero (Fig.2). Analytical expression for the voltage can be obtained within a point-dipole approximation and using the image charge method. The longitudinal voltage drop along the direction of the DW motion is obtained as,

$$V_x = \pi \frac{\hbar}{e} \frac{v_y}{w}, \tag{11}$$

with v_y being the magnitude of the transverse velocity.

This longitudinal voltage drop is proportional to the transverse speed, and inversely proportional to the wire width. The result is universal in the sense that it is independent of the detailed wall profile including its polarization and vorticity. In fact, as confirmed by our numerical calculations, this result is exact beyond the point-dipole approximation as long as the core is contained within the width and is far from the two ends of the sample. Measurement of this universal result may provide clear characterization of the vortex motion.

The average value of this voltage depends on the average frequency of the wall transformation. Recent experiments and simulations [31, 32] suggest that for narrow nanowires, this frequency is approximately the Larmor frequency. So $\bar{v}_y/w = \gamma H/\pi$, where $\bar{v}_y$ is time averaged transverse speed, γ is the gyromagnetic ratio and H is the applied magnetic field strength. In this case,

$$\bar{V}_x = \frac{\hbar}{e}\gamma H, \tag{12}$$

which means the DC part of the voltage signal is universal and only depends on the applied magnetic field. This result is in good agreement with the voltage obtained by solving Poisson equation directly (Fig.3). Here we also expect there are small oscillations around this DC signal with the Larmor frequency.

The motion of the vortex also induces a transverse voltage, which can also be calculated from the Poisson equation. For a vortex at the center of the wire, the transverse voltage at the longitudinal position of the vortex is found to be

$$V_y = \pi pq \frac{\hbar}{e} \frac{v_x}{w}. \tag{13}$$

which can be measured through a pair of lateral leads. At low fields, this voltage is a constant, and one should observe a pulse of transverse voltage with the above peak

value with its width determined by the wall speed and lead width. Strong oscillations occur within this pulse above the breakdown field when the vortex or antivortex executes complicated motion.

So far we have only considered the spin majority carriers and the sample being disorder free. In real situation, for adiabatic approximation to be valid, we need $J/(\hbar/\tau) \gg 1$, where τ is the carrier mean free time between elastic scattering events [34]. This condition ensures the probability of spin flip due to collision broadening is negligible. For Permalloy thin films at room temperature, this condition still holds for spin majority carriers but breaks down for minority carriers. Therefore the above Berry phase effects disappear for minority carriers because their phases are randomized due to scattering.

Finally, we give an estimation of the extra voltage due to nonadiabatic or dissipative effects. Originally obtained from force balance considerations [5], this contribution has been related to the nonadiabatic spin transfer torque recently [18]. This voltage drop can be written as $V_x^{na} = 2M_s R_0 \mu_i^{-1} v_x$, where R_0 is the ordinary Hall coefficient and μ_i, called the intrinsic wall mobility, is a measure of the electrons' contribution to the viscous damping force on the domain wall. For Permalloy thin films, $M_s = 8 \times 10^5 \mathrm{A/m}$, $R_0 = -1.4 \times 10^{-10} \mathrm{m}^3/\mathrm{C}$ and $\mu_i \simeq 2\mathrm{m}^2/\mathrm{C}$. Then V_x^{na} is at least 10 times smaller than the adiabatic voltage above breakdown. However, it is the dominant contribution to the longitudinal voltage below breakdown.

In summary, we have proposed a general theory for studying electron dynamics in the presence of moving local spin textures. We find that the variation of local spin textures gives rise to two topological fields acting on the conduction electrons as driving forces. Using this formalism, we reproduce the result for transverse wall motion. Moreover, universal results are obtained for the voltage induced by a moving vortex wall and its measurement can be used for detecting the domain wall motion. Finally, we estimate the nonadiabatic contributions to the voltage drop which shall be important below Walker breakdown.

The authors would like to thank Changhai Xu, Weidong Li, Chih-Piao Chuu, Wang Yao, Dennis P. Clougherty, Shufeng Zhang, Geoffrey S. D. Beach, Maxim Tsoi and James L. Erskine for valuable discussions. SY was supported by NSF DMR-0404252, DX was supported by NSF DMR-0606485, and QN by the Welch Foundation and DOE (DE-FG03-02ER45958).

[1] J. F. Gregg, W. Allen, K. Ounadjela, M. Viret, M. Hehn, S. M. Thompson, and J. M. D. Coey, Phys. Rev. Lett. **77**, 1580 (1996).
[2] G. Tatara and H. Fukuyama, Phys. Rev. Lett. **78**, 3773 (1997).
[3] R. P. van Gorkom, A. Brataas, and G. E. W. Bauer, Phys. Rev. Lett. **83**, 4401 (1999).
[4] V. K. Dugaev, J. Barnas, A. Łusakowski, and Ł. A. Turski, Phys. Rev. B **65**, 224419 (2002).
[5] L. Berger, J. Appl. Phys. **55**, 1954 (1984).
[6] G. Tatara and H. Kohno, Phys. Rev. Lett. **92**, 086601 (2004).
[7] Z. Li and S. Zhang, Phys. Rev. B **70**, 024417 (2004); Phys. Rev. Lett. **92**, 207203 (2004). S. Zhang and Z. Li, Phys. Rev. Lett. **93**, 127204 (2004). Z. Li, J. He, and S. Zhang, J. Appl. Phys. **99**, 08Q702 (2006).
[8] A. Thiaville, J. Miltat and J. Vernier, J. Appl. Phys. **95** 7049 (2004). A. Thiaville, Y. Nakatani, J. Miltat, and Y. Suzuki, Europhys. Lett. **69**, 990 (2005).
[9] S. E. Barnes and S. Maekawa, Phys. Rev. Lett. **95**, 107204 (2005).
[10] J. Ohe and B. Kramer, Phys. Rev. Lett. **96**, 027204 (2006).
[11] M. Benakli, J. Hohlfeld, and A. Rebei,arXiv:0708.2412v1.
[12] A. Yamaguchi, T. Ono, S. Nasu, K. Miyake, K. Mibu, and T. Shinjo, Phys. Rev. Lett. **92**, 077205 (2004).
[13] M. Kläui, P.-O. Jubert, R. Allenspach, A. Bischof, J. A. C. Bland, G. Faini, U. Rüdiger, C. A. F. Vaz, L. Vila, and C. Vouille, Phys. Rev. Lett. **95**, 026601 (2005).
[14] G. S. D. Beach, C. Knutson, C. Nistor, M. Tsoi, and J. L. Erskine, Phys. Rev. Lett. **97**, 057203 (2006).
[15] M. Hayashi, L. Thomas, Ya. B. Bazaliy, C. Rettner, R. Moriya, X. Jiang, and S. S. P. Parkin , Phys. Rev. Lett. **96**, 197207 (2006).
[16] L. Berger, Phys. Rev. B **33**, 1572 (1986).
[17] S. E. Barnes, J. Ieda and S. Maekawa, Appl. Phys. Lett. **89**, 122507 (2006). S. E. Barnes and S. Maekawa, Phys. Rev. Lett. **98**, 246601 (2007).
[18] R. A. Duine, Phys. Rev. B **77**, 014409 (2008).
[19] W. M. Saslow, Phys. Rev. B **76**, 184434 (2007).
[20] M. V. Berry, Proc. R. Soc. London, Ser. A **392**, 45 (1984).
[21] H. B. Braun and D. Loss, Phys. Rev. B **53**, 3237 (1996).
[22] Y. B. Bazaliy, B. A. Jones, and S. C. Zhang, Phys. Rev. B **57**, R3213 (1998).
[23] R. D. Mcmichael and M. J. Donahue, IEEE Trans. Magn. **33**, 4167 (1997).
[24] M. Kläui, C. A. F. Vaz and J. A. C. Bland, L. J. Heyderman, F. Nolting, A. Pavlovska, E. Bauer, S. Cherifi, S. Heun, and A. Locatelli, Appl. Phys. Lett. **85**, 5637 (2004).
[25] G. Sundaram and Q. Niu, Phys. Rev. B **59**, 14915 (1999).
[26] A. P. Malozemoff and J. C. Slonczewski, *Magnetic Domain Walls in Bubble Materials* (Academic Press, New York, 1979).
[27] Private communication with S. Zhang.
[28] J. Shibata, Y. Nakatani, G. Tatara, H. Kohno, Y. Otani, Phys. Rev. B **73**, 020403(R) (2006).
[29] J. He, Z. Li and S. Zhang, Phys. Rev. B **73**, 184408 (2006).
[30] Y. Nakatani, A. Thiaville and J. Miltat, Nature Mater. **2**, 521 (2003).
[31] J.-Y. Lee, K.-S. Lee, S. Choi, K. Y. Guslienko, and S.-K. Kim, arXiv:cond-mat/07062542. J.-Y. Lee, K.-S. Lee, S. Choi, K. Y. Guslienko, and S.-K. Kim, Phys. Rev. B **76**, 184408 (2007).
[32] M. Hayashi, L. Thomas, C. Rettner, R. Moriya and S. S. P. Parkin, Nature Physics **3**, 21 (2007).
[33] G. S. D. Beach, C. Nistor, C. Knutson, M. Tsoi, and J. L. Erskine, Nat. Mater. **4**, 741 (2005).

[34] M. Popp, D. Frustaglia, and K. Richter, Phys. Rev. B **68**, 041303(R) (2003).